

Low Frequency Spin Dynamics in the CeMIn₅ Materials

N. J. Curro, J. L. Sarrao, and J. D. Thompson

Condensed Matter and Thermal Physics, Los Alamos National Laboratory, Los Alamos, NM 87545, USA

P. G. Pagliuso

Instituto de Física “Gleb Wataghin”, UNICAMP, 13083-970, Campinas-SP, Brazil

Š. Kos, Ar. Abanov, and D. Pines

Theoretical Division, Los Alamos National Laboratory, Los Alamos, NM 87545, USA

(Dated: October 30, 2018)

We measure the spin lattice relaxation of the In(1) nuclei in the CeMIn₅ materials, extract quantitative information about the low energy spin dynamics of the lattice of Ce moments in both CeRhIn₅ and CeCoIn₅, and identify a crossover in the normal state. Above a temperature T^* the Ce lattice exhibits “Kondo gas” behavior characterized by local fluctuations of independently screened moments; below T^* both systems exhibit a “Kondo liquid” regime in which interactions between the local moments contribute to the spin dynamics. Both the antiferromagnetic and superconducting ground states in these systems emerge from the “Kondo liquid” regime. Our analysis provides strong evidence for quantum criticality in CeCoIn₅.

PACS numbers: 76.60.-k, 75.20.-g, 75.25.+z, 71.27.+a

The CeMIn₅ heavy fermion materials possess a rich phase diagram revealing a fascinating interplay between the antiferromagnetic behavior of incompletely screened Ce local moments, an unconventional normal state, and superconducting behavior of the heavy electrons that is reminiscent of that found in the cuprates [1, 2]. The non-Fermi liquid behavior of the itinerant heavy electrons and the possible d-wave symmetry of their superconducting state has led to the proposal that the superconducting pairing mechanism arises from their coupling to spin fluctuations [1, 3, 4, 5, 6]. In this Letter, we consider the information about the coupled system of Ce local moments and itinerant heavy electrons that can be derived from Nuclear Magnetic Resonance (NMR) experiments on the spin lattice relaxation rate (T_1^{-1}) of the In(1) nuclei located in the plane of the Ce moments. We show that the In(1) nuclei are strongly coupled to their four nearest neighbor Ce spins by an anisotropic hyperfine interaction, and that the resulting anomalous behavior of $T_1 T$ provides important information on the low frequency dynamics of the lattice of Ce spins, and the quasi-particles to which they couple. Because the coupling is anisotropic, it does not vanish for antiferromagnetically correlated Ce moments, so that T_1^{-1} provides valuable information on the dynamics of their magnetic ordering, as well as on the influence of Kondo screening of the moments on their relaxation rate, and departures from Kondo behavior at low temperatures [7, 8]. We present our results for both the antiferromagnet CeRhIn₅ and the superconductor CeCoIn₅.

Previous reports of T_1^{-1} in CeIrIn₅ and CeCoIn₅ by other authors have attributed an unusual temperature dependence of T_1^{-1} in the normal state to antiferromagnetic fluctuations up to room temperature [9, 10]. We show in both CeRhIn₅ and CeCoIn₅ that above a temperature T^* of the order 10K, T_1^{-1} is dominated by *lo-*

cal fluctuations of the Ce moments. Below T^* the \mathbf{q} -independent local moment contribution to T_1^{-1} becomes temperature independent, and a second \mathbf{q} and T dependent component emerges. We identify this emergent component with the heavy electrons, that is the itinerant component of the Ce 4f electrons arising from their coupling to one another and to the conduction electrons. This extra contribution to the relaxation agrees quantitatively with inelastic neutron scattering (INS) results in CeRhIn₅, and suggests that the antiferromagnetic correlations in CeCoIn₅ are primarily 2D, and that in the absence of superconductivity one would have a quantum critical point corresponding to a transition from Fermi liquid to antiferromagnetic behavior at $T = 0$.

In order to develop a model for the hyperfine coupling in the CeMIn₅ materials, it is necessary to determine the number of spin degrees of freedom, and the hyperfine couplings to each degree of freedom. For all three materials (M=Rh, Ir, Co), the bulk susceptibility χ is dominated at high temperatures by localized Ce moments, and can be adequately fit by an expression for these moments in a tetragonal crystalline electric field (CEF) [11, 12, 13, 14, 15]. Neutron diffraction (ND) in the ordered state of CeRhIn₅ indicates that the magnetism is localized on the Ce sites, albeit with reduced moments [16]. The reduced moment plausibly reflects some degree of hybridization with incomplete screening of the Ce moment in the CEF ground state doublet. (For the CEF scheme measured in [15] the ground state doublet has a moment of $0.92\mu_B$, whereas the measured moment is $0.74\mu_B$ [16, 17, 18].) The magnetic shifts of the high symmetry In(1) site in CeRhIn₅, presented in Fig. (1), are linear in χ in the paramagnetic state. If the main contribution to the magnetic shift arises from the localized Ce moments, then $K_\alpha = K_{0,\alpha} + \beta_\alpha \chi_\alpha$, where β_α is an effective hyperfine coupling and $\alpha = c, ab$. Note that

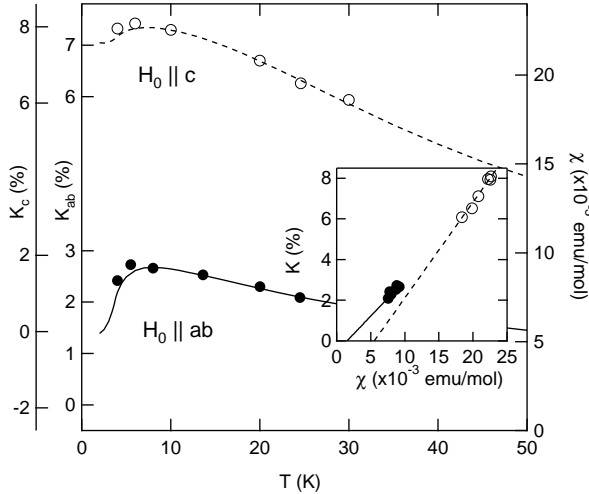


FIG. 1: The magnetic shift of In(1) in CeRhIn₅ (circles) and the bulk susceptibility (lines) versus temperature. The inset shows K_c versus χ_α . The solid (open) circles and solid (dashed) lines are for $H \parallel ab$ ($H \parallel c$).

the hyperfine coupling is anisotropic ($\beta_c = 26.4\text{kOe}/\mu_B$, $\beta_{ab} = 19.6\text{kOe}/\mu_B$), and the size of these hyperfine couplings are more than an order of magnitude greater than typical dipolar fields ($\sim 1\text{kOe}/\mu_B$), so the In(1) must be coupled to the Ce via an anisotropic transferred hyperfine coupling of electronic origin.

We postulate that the In(1) nucleus is coupled to each of the four nearest neighbor Ce spins through a tensor $\tilde{\mathbf{A}} = \{A_{||}, A_{\perp}, A_c\}$, where the principal axes lie parallel and perpendicular to the Ce-In(1) bond axis in the ab plane, and along the c axis:

$$\mathcal{H} = \gamma\hbar \sum_{i \in \text{n.n.}} \mathbf{I} \cdot \tilde{\mathbf{A}}_i \cdot \mathbf{S}_i. \quad (1)$$

Here γ is the gyromagnetic ratio, \mathbf{I} is the nuclear spin of the In(1), \mathbf{S}_i is the spin on the i^{th} Ce, and the sum is over the four nearest neighbor Ce sites. Note that there should also exist a direct hyperfine coupling between the In nuclei and the conduction electrons. However, the fact that T_1^{-1} drops by almost two orders of magnitude below T_N suggests that this coupling is small compared to the coupling between the nuclei and the Ce moments. For notational simplicity, we define A_{ab} and x as $A_{||, \perp} = A_{ab}(1 \pm x)$. Using Eq. (1) one can show that $K_c = 4A_c\chi_c$ and $K_{ab} = 4A_{ab}\chi_{ab}$; using the slopes of K_α versus χ_α given above, we have $A_{ab} = 4.9\text{kOe}/\mu_B$ and $A_c = 6.6\text{kOe}/\mu_B$. The parameter x can be determined from the internal field in the antiferromagnetic state. The moments are localized on the Ce sites, with the structure given by: $\mathbf{S}(\mathbf{r}_i) = S_0 \cos(\pi x/a) \cos(\pi y/a) \{\cos(q_0 z), \sin(q_0 z), 0\}$, where $S_0 = 0.74\mu_B$, and $q_0 = 0.297\frac{2\pi}{c}$ [16, 17, 18, 19]. For this structure, the internal field is given by: $\mathbf{H}_{\text{int}} = 2A_{ab}xS_0 \{\sin(q_0 z), \cos(q_0 z), 0\}$. The measured internal

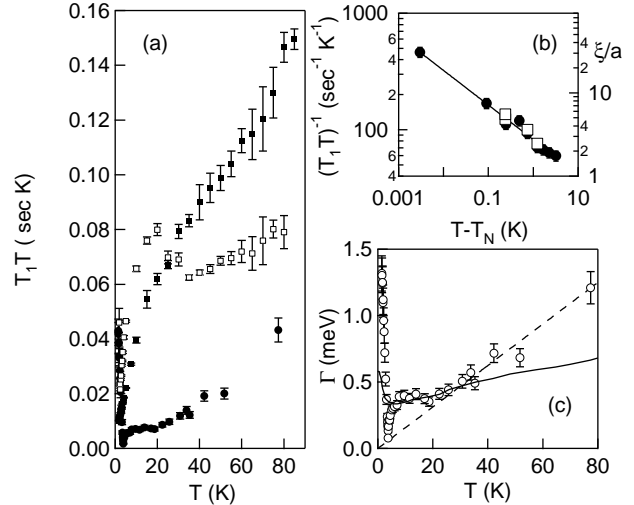


FIG. 2: (a) T_1T versus T in CeRhIn₅ and CeCoIn₅; the CeRhIn₅ data for $T > 20\text{K}$ are taken from [20] (CeRhIn₅ NQR (●), CeCoIn₅ $H_0 \parallel c$ (solid squares), and $H_0 \parallel ab$ (open squares)). (b) $(T_1T)^{-1} - 111.43\text{sec}^{-1}\text{K}^{-1}$ (●) and ξ/a (open squares, ref [7]) vs. $T - T_N$ in CeRhIn₅, where the solid line is a fit as described in the text. (c) Γ vs. T for CeRhIn₅. The dashed line is a linear fit to the data above 20K, and the solid line is taken from [8] using $T_0 = 5\text{K}$.

field H_{int} at the In(1) site for $T \ll T_N$ is 1.7 kOe [19], which corresponds to a value $x = 0.12$.

The spin lattice relaxation of the In(1) nuclei is determined by the fluctuations of the Ce spins, and is given by the Fourier component of $\langle \mathcal{H}(t)\mathcal{H}(0) \rangle$ at the Larmor frequency, where the time dependence arises from the fluctuations of the Ce spins \mathbf{S}_i . Moriya showed that the spin lattice relaxation rate can be expressed in the general form [21]:

$$\frac{1}{T_1T} = \frac{\gamma^2 k_B}{2} \lim_{\omega \rightarrow 0} \sum_{\mathbf{q}, \alpha} F_\alpha^2(\mathbf{q}) \frac{\chi_{ab}''(\mathbf{q}, \omega)}{\omega} \quad (2)$$

where α is summed over the two directions perpendicular to the applied static field. Here $F_\alpha^2(\mathbf{q})$ are form factors, $\chi_\alpha(\mathbf{q}, \omega)$ is the dynamical susceptibility, and the sum is over the Brillouin zone. The form factors are the spatial Fourier transforms of the coupling in Eq. (1), and are given by:

$$\begin{aligned} F_{ab}^2(\mathbf{q}) &= 16A_{ab}^2 \cos^2\left(\frac{q_x a}{2}\right) \cos^2\left(\frac{q_y a}{2}\right) \\ &\quad + 16A_{ab}^2 x^2 \sin^2\left(\frac{q_x a}{2}\right) \sin^2\left(\frac{q_y a}{2}\right) \end{aligned} \quad (3)$$

$$F_c^2(\mathbf{q}) = 16A_c^2 \cos^2\left(\frac{q_x a}{2}\right) \cos^2\left(\frac{q_y a}{2}\right). \quad (4)$$

Since $F_{ab}^2(\mathbf{q}) > 0$ for all \mathbf{q} , T_1^{-1} will pick up fluctuations at all wavevectors. In particular, the In(1) is sensitive to the critical slowing down of the spin fluctuations above T_N .

We now can determine quantitatively the low frequency spin spectrum of CeRhIn₅. As may be seen in Fig. (2), T_1T varies quadratically with T for $T > 20$ K, which is what might have been anticipated for a collection of independent Ce moments that are weakly coupled to the conduction electrons via an interaction $\mathcal{H} = J\sigma \cdot \mathbf{S}$. To see this we note that the susceptibility of the local moments is given by:

$$\chi_L(\omega) = \frac{\chi_0(T)}{1 - i\omega/\Gamma(T)}, \quad (5)$$

where $\chi_0(T)$ is the bulk susceptibility ($\sim 1/T$ for $T > 20$ K), $\Gamma(T) = \pi J^2 N^2(0) k_B T$, and $N(0)$ is the electronic density of states at E_F . From Eqs. (2,3,5) we then have:

$$(T_1T)^{-1} = 4\gamma^2 k_B A_{ab}^2 (1 + x^2) \chi_0(T) / \Gamma(T) \sim T^{-2}. \quad (6)$$

Fig. (2c) shows $\Gamma(T)$ as a function of temperature. Note that $\Gamma \sim T$ for $T > 20$ K, with a slope determined by $JN(0) \sim 0.24$. Although INS data of $\Gamma(T)$ is unavailable in this material, Bao and coworkers have estimated that $\Gamma \ll 3$ meV for $T < 7$ K [7].

We interpret the crossover at 20K to an almost constant value of Γ as reflecting the onset of Kondo screening of the local moments. The relaxation of independently screened local moments, a "Kondo gas", has been calculated by Cox *et al.* [22], who find $\Gamma(T) = T_0 f(T/T_0)$ where f is a universal function reflecting a temperature dependent effective coupling, and T_0 is proportional to the Kondo temperature. For $T > T_0$, Qachaou *et al.* have shown that this scaling behavior holds for several mixed-valent and heavy electron materials [23]. As may be seen in Figs. (2c) and (3), a good fit to the experimental data may be obtained with $T_0 = 5$ K over the range 8K < $T < 40$ K.

Below $T^* \sim 8$ K one begins to see the "Kondo liquid" expected when the interaction between the Ce local moments induced by their coupling to the conduction electrons plays a dominant role in the relaxation of the moments. Indeed, for $T_N < T < T^*$, T_1^{-1} shows a strong divergence associated with the critical slowing down of the spin fluctuations of this Kondo liquid. In this region the susceptibility takes the form:

$$\chi_{AF}(\mathbf{q}, \omega) = \frac{\alpha \xi^2(T) \mu_B^2}{1 + \xi^2(T)(\mathbf{q} - \mathbf{Q})^2 - i\omega/\omega_{sf}(T)}, \quad (7)$$

which adequately describes the INS data [7]. Here α is a temperature independent constant, and $\omega_{sf} \sim 1/\xi^z$, where z is the dynamical scaling constant. In the mean field regime, $z = 2$ and we have $(T_1T)^{-1} = (T_1T)_0^{-1} + (T_1T)_{AF}^{-1}$, where $(T_1T)_0^{-1}$ is the \mathbf{q} -independent, "local", contribution assumed constant below T^* , and $(T_1T)_{AF}^{-1}$ is the contribution from the antiferromagnetic fluctuations. The latter is given by $(T_1T)_{AF}^{-1} \approx \gamma^2 A_{ab}^2 x^2 k_B \alpha \mu_B^2 / 2\pi^2 \omega_{sf} \xi$, where we have assumed 3D fluctuations, and that the correlation length along the c direction, $\xi_c \sim \xi_{ab} \sim \xi$. If we assume mean field

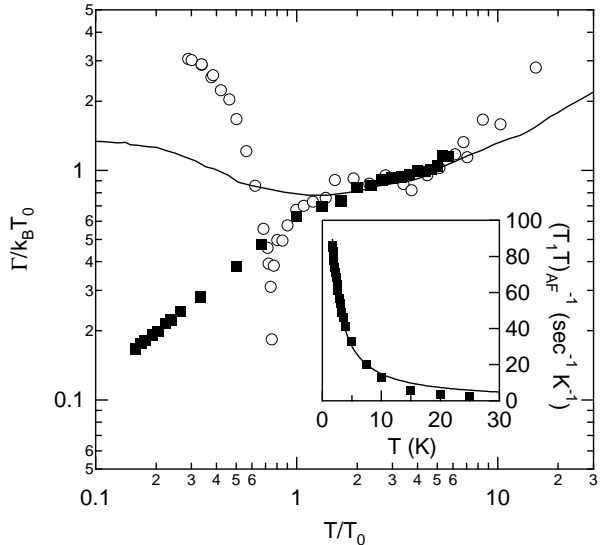


FIG. 3: $\Gamma(T)/k_B T_0$ versus T/T_0 . (o) CeRhIn₅ with $T_0 = 5$ K, and (solid squares) CeCoIn₅ with $T_0 = 17$ K. The solid line is from Cox [8]. The inset shows the build-up of antiferromagnetic correlations below ~ 30 K follows the $1/T$ behavior (solid line) described in the text, and extend to $T_c = 1.8$ K, the transition temperature for the 5T magnetic field used in this experiment.

behavior, then $(T_1T)_{AF}^{-1} \sim \xi(T)$. Fig. (2b) shows $(T_1T)^{-1} - (T_1T)_0^{-1}$ versus T , where $(T_1T)_0 = 0.00897$ sec K. The solid line is a fit to $\xi \sim (T - T_N)^{-\nu}$, where $\nu = 0.30 \pm 0.05$. As seen in Fig. (2b), the temperature dependence of the NMR measurements agrees well with INS measurements of ξ . Note that for a single critical point, a mean field analysis gives $\nu = \beta = 1/2$ ($M_{\text{sublattice}} \sim (T_N - T)^\beta$). The fact that we observe $\nu \sim 0.3$ suggests that either the point $T_N(H = 0)$ is a multicritical point, or that fluctuations change the exponents. The former is a plausible explanation for the critical exponent $\beta = 0.25$ observed in NMR and ND measurements [16, 19], and is consistent with the phase diagram in [24].

We next consider the superconductor CeCoIn₅. In order to deduce the hyperfine tensor, three independent experimental quantities are required. From the Knight shifts in this material measured in [12] we have $A_{ab} = 3.0$ kOe/ μ_B and $A_c = 2.2$ kOe/ μ_B . As discussed there, the Knight shift measurements show that for $T < 50$ K A_c vanishes whereas A_{ab} does not change; this behavior is reflected as the anomalous rise in the T_1T data below 40K in Fig. (2a) for $H_0 \parallel ab$. A direct measurement of the parameter x is lacking since there is no magnetic order [25]. For concreteness we assume $x = 0.12$, as in CeRhIn₅. Fig. (3) shows $\Gamma(T)/k_B T_0$ versus T/T_0 for CeCoIn₅ and CeRhIn₅, where $T_0 = 5$ K for CeRhIn₅, and $T_0 = 17$ K, for CeCoIn₅. The CeCoIn₅ data were determined using the T_1T data for $H_0 \parallel c$. For different values of x , the overall magnitude of the $\Gamma(T)$ data, and hence

T_0 , will change by at most a factor of two, but the overall temperature dependence will be the same and the conclusions will not change.

Note that in both materials the data scale with the Cox formula for $T > T^* \approx 1.5T_0$, however below this temperature $\Gamma(T)$ is less than the Cox prediction. As was the case for CeRhIn₅, $\Gamma(T)$ drops markedly below the Cox "Kondo gas" prediction below T^* , a change we can identify with the onset of a "Kondo liquid" regime in which the interactions between the local moments gives rise to a new physical regime. We suggest that just as in the Rh material, T^* in the Co material also marks the onset of antiferromagnetic correlations, and proceed to analyze the data in CeCoIn₅ below T^* in the same fashion as in CeRhIn₅.

The inset of Fig. (3) shows $(T_1T)_{AF}^{-1} = (T_1T)^{-1} - (T_1T)_0^{-1}$ versus T , where we have taken $(T_1T)_0 = 0.0793$ sec K, the value at 30K. The solid line is $(T - T_N)^{-1}$, with $T_N = 0$. Importantly, this result suggests that in the absence of superconductivity CeCoIn₅ would order magnetically at $T \sim 0$, so that in this material one has a quantum critical point that is obscured by superconductivity [26]. Quantum criticality is also consistent with the non-Fermi liquid behavior seen in the normal state [27].

It is also consistent with experiments at fields $H > H_{c2}$ that show the specific heat increases at low temperatures as though there were an ordering temperature at $T \approx 0$ [2]. The temperature dependence of $(T_1T)_{AF}^{-1}$ is significant. In the CeRhIn₅, $(T_1T)_{AF,3D}^{-1} \sim \xi$, as expected for 3D fluctuations. On the other hand, for quasi-2D fluctuations $(T_1T)_{AF,2D}^{-1} \sim \omega_{sf}^{-1} \sim \xi^2$. In fact, the data in CeCoIn₅ are best understood in a picture of 2D fluctuations, where $\omega_{sf} \sim T$, which is exactly the result observed in the cuprates above the pseudogap temperature [28]. In light of the behavior observed in CeRhIn₅ such correlations provide a natural explanation of the suppression of Γ , as well as a possible mechanism for the d-wave superconductivity [29]. Indirect evidence for such correlations has been seen in [14]. Measurements of Knight shift and T_1^{-1} under pressure and as a function of doping should prove invaluable to understanding the evolution of these antiferromagnetic correlations as the ground state changes from antiferromagnetic to superconducting.

We thank P. C. Hammel, C. P. Slichter, W. Bao, A. Balatsky, C. Varma, J. Lawrence, Z. Fisk, and Y. Bang for useful discussions. This work was performed under the auspices of the U.S. Department of Energy.

-
- [1] H. Hegger, C. Petrovic, E. G. Moshopoulou, M. F. Hundley, J. L. Sarrao, Z. Fisk, and J. D. Thompson, Phys. Rev. Lett. **84**, 4986 (2000).
- [2] C. Petrovic, P. G. Pagliuso, M. F. Hundley, R. Movshovich, J. L. Sarrao, J. D. Thompson, Z. Fisk, and P. Monthoux, Journal Of Physics-Condensed Matter **13**, L337 (2001).
- [3] N. D. Mathur, F. M. Grosche, S. R. Julian, I. R. Walker, D. M. Freye, R. K. W. Haselwimmer, and G. G. Lonzarich, Nature **394**, 39 (1998).
- [4] A. V. Chubukov, D. Pines, and J. Schmalian, cond-mat/0201140.
- [5] Y. Bang, I. Martin, and A. V. Balatsky, Phys. Rev. B **66**, 224502 (2002).
- [6] K. Miyake, S. Schmitt-Rink, and C. Varma, Phys. Rev. B **34**(9), 6554 (1986).
- [7] W. Bao, et al., Phys. Rev. B **65**, 100505 (2002).
- [8] D. Cox, N. Bickers, and J. Wilkins, J. Appl. Phys. **57**, 3166 (1985).
- [9] G. Zheng, et al., Phys. Rev. Lett. **86**, 4664 (2001).
- [10] Y. Kohori, et al., Phys. Rev. B **64**, 134526 (2001).
- [11] T. Takeuchi, et al., J. Phys. Soc. Jpn. **70**, 877 (2001).
- [12] N. J. Curro, et al., Phys. Rev. B **64**, 180514 (2001).
- [13] P. G. Pagliuso, N. O. Moreno, N. J. Curro, J. D. Thompson, M. F. Hundley, L. L. Sarrao, and Z. Fisk (2002), to appear in Physica B.
- [14] S. Nakatsuji, et al., Phys. Rev. Lett. **89**, 106402 (2002).
- [15] A. Christianson, A. Lacerda, M. Hundley, P. Pagliuso, and J. Sarrao, Physical Review B **6605**(5), 4410 (2002).
- [16] W. Bao, et al., Phys. Rev. B **62**, 14 621 (2001).
- [17] W. Bao, et al., Phys. Rev. B **63**, 219901 (2001).
- [18] A. Llobet (2002), private communication.
- [19] N. J. Curro, P. C. Hammel, P. G. Pagliuso, J. L. Sarrao, J. D. Thompson, and Z. Fisk, Phys. Rev. B **62**, R6100 (2000).
- [20] et al., Eur. Phys. B **18**, 601 (2000).
- [21] T. Moriya, J. Phys. Soc. Jpn. **18**, 516 (1963).
- [22] E. Kim, M. Makivic, and D. L. Cox, Phys. Rev. Lett. **75**, 2015 (1995).
- [23] A. Qachaou, et al., J. Mag. Magn. Mat. **63-64**, 635 (1987).
- [24] A. Cornelius, P. Pagliuso, M. Hundley, and J. Sarrao, Phys. Rev. B **6414**(14), 4411 (2001).
- [25] In principle, one can extract x by measuring the anisotropy of T_1 for $T > T^*$. Using Eqs. (2-3,6) $\frac{(T_1^{-1})_{ab}}{(T_1^{-1})_c} = \frac{1}{2} + \frac{A_c^2}{2A_{ab}^2(1+x^2)} \frac{\chi_c(T)}{\chi_{ab}(T)}$. We find this ratio goes to 1/2 for $T \rightarrow 0$, reflecting the fact that A_c vanishes. However, no physically reasonable values of x exist that satisfy the data for $T >> 50$ K, which probably signifies that $\Gamma(T)$ is anisotropic.
- [26] V. Sidorov, M. Nicklas, P. Pagliuso, J. Sarrao, Y. Bang, A. Balatsky, and J. Thompson, Phys. Rev. Lett. **8915**(15), 7004 (2002).
- [27] A. Bianchi, et al., Phys. Rev. Lett. **8913**(13), 7002 (2002).
- [28] R. Corey, et al., Phys. Rev. B **53**(9), 5907 (1996).
- [29] P. Monthoux and G. G. Lonzarich, Phys. Rev. B **63**, 054529/1 (2001).